Feng Gao
Department of Civil and Environmental Engineering, McCormick School of Engineering and Applied Science, Northwestern University, 2145 Sheridan Road, Evanston, IL 60208
e-mail: feng-gao@northwestern.edu

Jianmin Qu
Department of Civil and Environmental Engineering, McCormick School of Engineering and Applied Science, Northwestern University, 2145 Sheridan Road, Evanston, IL 60208; Department of Mechanical Engineering, McCormick School of Engineering and Applied Science, Northwestern University, 2145 Sheridan Road, Evanston, IL 60208
e-mail: j-qu@northwestern.edu

Matthew Yao
Rockwell Collins Inc, 400 Collins Rd NE, Cedar Rapids, IA 52498
e-mail: myao@rockwellcollins.com

Electrical Contact Resistance at the Carbon Nanotube/Pd and Carbon Nanotube/Al Interfaces in End-Contact by First-Principles Calculations

Reported in this paper is a quantum mechanics study on the electronic structure and contact resistance at the interfaces formed when an open-end single-walled carbon nanotube (CNT) is in end-contact with aluminum (Al) and palladium (Pd), respectively. The electronic structures are computed using a density functional theory (DFT), and the transmission coefficient is calculated using a nonequilibrium Green's function (NEGF) in conjunction with the DFT. The current–voltage relation of the simulating cell is obtained by using the Landauer–Buttiker formula, from which the contact resistance can be determined. Our results show that the electronic structure and electron transport behavior are strongly dependent on the electrode. It is found that the CNT/Pd interface has a weaker bond than the CNT/Al interface. However, the CNT/Pd interface shows a lower electrical contact resistance. [DOI: 10.1115/1.4004095]

Keywords: carbon nanotube, first-principles, electronic structure, contact resistance

Introduction

Carbon nanotube (CNT) is one of the most promising candidates in nanoscale electronic devices due to their size, structural strength, and excellent electrical and thermal properties [1]. It has been reported that an individual semiconducting CNT can operate either as a conventional metal-oxide semiconductor field-effect transistor or an unconventional Schottky barrier transistor when it makes a contact with a metal electrode. Thus, in potential electronic device applications, one of the key issues is the electrical contact resistance between semiconducting single-walled CNTs and the metallic electrodes [2].

Various metal electrodes, such as Ti, Pd, Cu, Au, Mo, Ni, and Pt, have been used to form the contact with CNTs. The electronic structures between CNTs and metal electrodes have also been studied by several researchers [3–9]. However, most of these studies mainly focused on the side-contact or embedded-contact between CNTs and metal electrodes. In practice, the end-contact between CNTs and electrodes is often needed for the potential electronic interconnections. In addition, recent research has shown that each wall of multiwalled CNTs contributes to the saturation current to obtain a very high current-carrying capacity, which means the multichannel electron transport could be achieved by opening multiwalled CNTs [10]. Thus, open-end CNT making end-contact with electrodes is gaining more attention from the industry. Although a few studies have been published on end-contact between CNT and metal electrodes [11–15], the interaction and the electron transport at the CNT/metal interface have not been fully studied yet.

Recently, the authors have reported a study on the electronic structure and electrical contact resistance between a semiconducting CNT (10, 0) in end-contact with copper (Cu), using first-principles calculations [16]. In this paper, the same methodology used in Ref. [16] will be adopted here to study the electronic structure and electrical contact resistance between a semiconducting CNT (10, 0) in end-contact with two other metal electrodes, namely, Al and Pd. The CNT tube is approximately 1 nm long. The metal electrode consisted of $6 \times 6 \times 6$ atoms. The scattering region is composed of CNT tube and two surface layers of electrode. The separation distance between CNT and metal electrode surface was determined by minimizing the interaction energy of the system. The local density of states near the CNT/metal interfaces are computed using a density functional theory (DFT), and the transmission coefficient is calculated using a nonequilibrium Green's function method in conjunction with the DFT. The current–voltage relation of the simulating cell is obtained by using the Landauer–Buttiker formula, from which the contact resistance is determined. Our results show that the electronic structure and electron transport behavior are strongly dependent on the electrode. It is found that the CNT/Pd interface has weaker bond than that of the CNT/Al interface. However, the CNT/Pd interface shows a lower electrical contact resistance.

First-Principles Simulations

The simulation cell is a two-probe system consisting of a semiconducting (10, 0) CNT with each end connected to a metal electrode (Al or Pd), see Fig. 1. The first-principles simulations were conducted using the ATK ToolKit code [17], in which the density functional theory with double-ξ plus polarization (DZP) basis sets is combined with the Keldysh nonequilibrium Green's function method to calculate the electronic structure and transport properties of the CNT/electrode contact system. All calculations were performed based on the generalized gradient approximation (GGA) with Perdew–Burke–Ernzerhof (PBE) pseudoatomic potentials [18].

An electrical voltage is prescribed across this two-probe system to generate a steady-state current. The electron transport direction along the tube axis is the z-direction and the other two orthogonal directions are the x- and y-directions. The contact resistance of the CNT/electrode interface is derived by the current–voltage relation

Contributed by the Electronic and Photonic Packaging Division of ASME for publication in the JOURNAL OF ELECTRONIC PACKAGING. Manuscript received January 17, 2010; final manuscript received April 2, 2011; published online July 1, 2011. Assoc. Editor: Cemal Basaran.

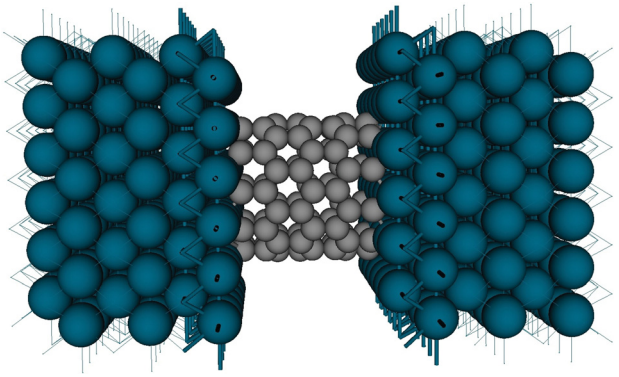

Fig. 1 Simulation cell of the two-probe system, CNT in end-contact with electrodes

(i.e., the *I–V* curve). The current–voltage relationship can be described by the Landauer–Buttiker formula [19], which relates the current to the voltage via the transmission probability $T(E, V)$.

$$I(V) = \frac{2e}{h}\int_{\mu_1}^{\mu_2} dET(E,V)[f(E-\mu_1) - f(E-\mu_2)] \tag{1}$$

where μ_1 and μ_2 are the chemical potential of left and right electrodes

$$f(E-\mu) = 1/\{1+\exp[E-\mu/k_B T_{\text{temp}}]\}$$

is the Fermi–Dirac distribution function, k_B is the Boltzmann constant, and T_{temp} denotes the temperature. The noncoherent charge transport processes are not considered, consequently coupling of different transverse modes are neglected. In this case, computation of the *I–V* relation amounts to the evaluation of the transmission function through independent $\mathbf{k}_{||}$ (surface-parallel direction reciprocal lattice vector point) channels and their integral over the 2D reciprocal unit cell Ω

$$T(E,V) = \frac{1}{\Omega}\int_{\bar{\Omega}} d\mathbf{k}_{||} T^{\mathbf{k}_{||}}(E,V) \tag{2}$$

where Ω is the area of the reference unit cell surface. In order to compute $T^{\mathbf{k}_{||}}$, the matrix version of the NEGF approach is employed, which is a well-developed general formalism to treat various nonequilibrium charge transport phenomena. The *k*-point sampling in Brillouin Zone integration parameters is 3, 3, and 50 in the *x*-, *y*-, and *z*-directions, respectively.

We note that when an electrical voltage is applied, the two-probe system will be out of its initial equilibrium state. To minimize such disturbance, a fully self-consistent calculation has been performed in our calculations. In order to achieve the convergence at high bias (e.g., 2 V), the voltage was increased incrementally. At each increment, the system configuration was stored and used as the initial configuration for the next increment.

Results and Discussions

To characterize the bond between the CNT and metal electrodes, the Mulliken population of the two-probe system was computed to separate the electron density into atomic contributions. The Mulliken overlap population (MOP) between the atoms for a particular orbital was then extracted to reveal the chemical bonding characteristics qualitatively [20].

Figures 2(*a*) and 2(*b*) present the MOP of the Al/CNT/Al and Pd/CNT/Pd systems, respectively. Only the scattering region that includes CNT and two layers of atoms on the metal surface is shown in these figures. Thicker lines represent higher bond strength. Note that the metallic bond between the metal atoms is not illustrated here.

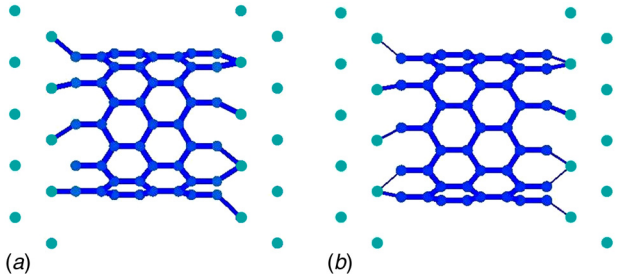

Fig. 2 Computed Mulliken Overlap population of electrode/CNT/electrode two-probe systems. Only the scattering region was presented herein. The green spheres represent the electrode atoms (Al or Pd), and blue spheres represent the C atoms in CNT: (*a*) Al/CNT/Al; (*b*) Pd/CNT/Pd.

It is seen that for both Al/CNT/Al and Pd/CNT/Pd systems, chemical bond is formed at the interface. Furthermore, the CNT/Al interface shows higher bond strength than that of the CNT/Pd interface. More specifically, our numerical results show that the average Al–C and Pd–C bond strengths are, respectively, ~90% and ~60% of the C–C bond strength in the CNT. The higher Al–C bonding may be attributed to the higher chemical reactivity of Al with C. For example, aluminum carbide will be formed when aluminum and carbon is heated up to 1000 °C [21].

The electronic structure at Fermi level is crucial to the electron transport at the interface. Figure 3 shows the computed local density of states (LDOS) at Fermi level ($E_F = 0$), which is projected onto a cross-section parallel to the CNT axis of the simulation

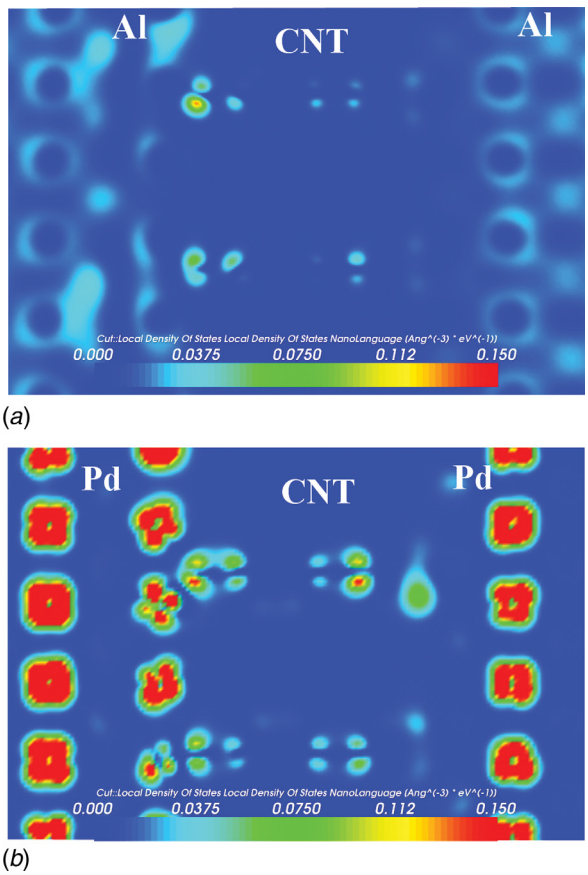

Fig. 3 Local density of states (LDOS) of CNT/metal end-contact systems: (*a*) Al/CNT/Al system; (*b*) Pd/CNT/Pd system

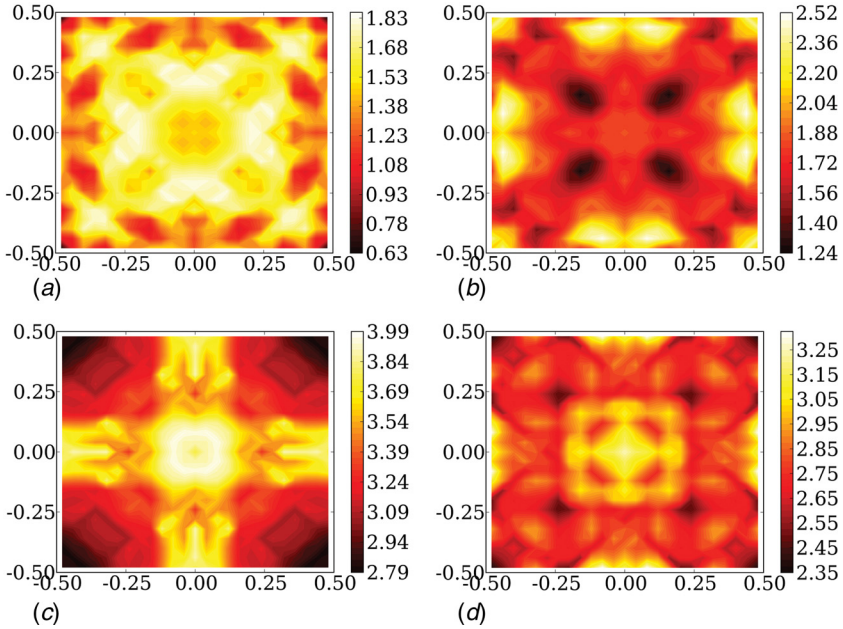

Fig. 4 Transmission contours at Fermi energy for Al/CNT/Al and Pd/CNT/Pd systems at different applied bias voltages: (*a*) Al/CNT/Al: 0.1 V; (*b*) Al/CNT/Al: 2 V; (*c*) Pd/CNT/Pd: 0.1 V; (*d*) Pd/CNT/Pd: 2 V

cell. The LDOS contours of metal atoms (e.g., Al or Pd) near the interface are significantly different from that of the bulk atoms. This implies that strong interactions have occurred at the CNT/metal interface. In addition, the C atoms at CNT/Pd interface exhibit more LDOS, compared to the CNT/Al interface. This implies a more active electron transport in the Pd/CNT/Pd system than in the Al/CNT/Al system. This conclusion will be confirmed later by the transmission coefficient calculations.

Figure 4 shows the detailed transmission coefficient relating to the *k*-sampling of Al/CNT/Al and Pd/CNT/Pd systems at the Fermi energy under two bias voltages, 0.1 V and 2.0 V. It is observed that the transmission coefficient is a function of applied bias voltages. Overall, the Pd/CNT/Pd system has a higher transmission coefficient than the Al/CNT/Al system. For the Al/CNT/Al system, the transmission coefficient near the Gamma (0, 0) *k*-point reaches its highest value under a lower bias (0.1 V), and its lowest value under a higher bias (2.0 V). For the Pd/CNT/Pd system, the transmission coefficient near the (0, 0) *k*-point reaches its highest value under both lower (0.1 V) and higher biases (2.0 V). Further investigations, such as the transmission eigenvalues at a certain energy level, and the bond coupling between the C and metal atoms, will be required to fully understand the dependence of the transmission coefficient on the applied bias voltages.

The transmission spectrum at various bias voltages can be calculated based on Eq. (2). The results are shown in Fig. 5. Again, it is seen that both systems, the transmission coefficient shows a strong dependence on the applied bias voltages. Furthermore, the Pd/CNT/Pd system exhibits higher transmissibility than the Al/CNT/Al system, particularly around the Fermi energy, which is consistent with the results in shown in Fig. 4.

Figure 6 shows the *I–V* curves for the two systems considered here. Note that at low applied voltage regime (0.0–0.1 V), the *I–V* relationship is linear [4,5,16]. Thus, the total resistance of the system can be computed via the Ohmic law. By averaging the data between 0 and 0.1 V, we found that the total electrical resistance of 8.2 kΩ for the Al/CNT/Al and 4.0 kΩ for Pd/CNT/Pd, respectively. It has been reported that the steady total resistance of a Al/CNT(5,5)/Al end-contact system is 7.39 kΩ [22], which is the same order as the Al/CNT(10, 0)/Al system in this study. As shown in Ref. [16], much of the total resistance is attributed to the contact resistance at the CNT/metal interfaces, since the total bulk resistance of the CNT and metal probes is negligible. Therefore, at each CNT/metal interface, the contact resistance is 4.1 kΩ and 2.0 kΩ for the CNT/Al and CNT/Pd interfaces, respectively.

If one assumes that the CNT/metal contact area is the open-end cross-section area of the CNT, and the CNT wall thickness is the van der Waals radius of a carbon atom (1.7 Å), the contact area can be computed. For the (10, 0) CNT with diameter 7.774 Å, the contact area so computed is 0.83 nm^2. Thus, the corresponding contact resistivity is ~3.4 kΩ nm^2 for the CNT/Al and 1.66 kΩ nm^2 for the CNT/Pd interfaces, respectively. In other words, the end-contact resistance is higher at the CNT/Al interface than at the CNT/Pd interface.

Intuitively, one would think that a stronger chemical bond at the interface should induce higher electron transmission across the interface, thus lead to lower contract resistance. This is not generally true in that the MOP results shows a higher chemical bonding at the CNT/Al interface than at the CNT/Pd interface, yet the CNT/Al interface show higher contact resistance than the CNT/Pd interface. In other words, there is generally no positive correlation between the charge transfer and the electron transport at the CNT/metal interface.

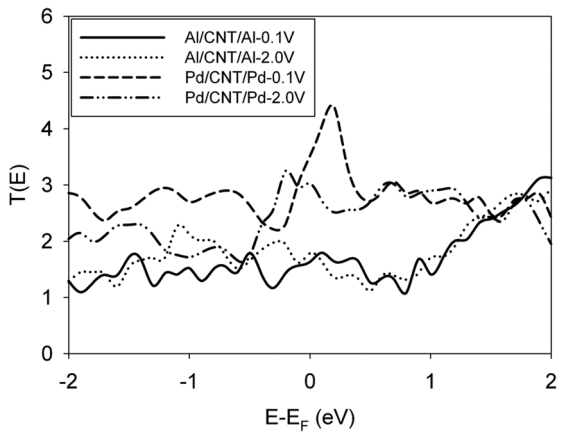

Fig. 5 Transmission spectrum of Al/CNT/Al and Pd/CNT/Pd systems at different prescribed bias voltages

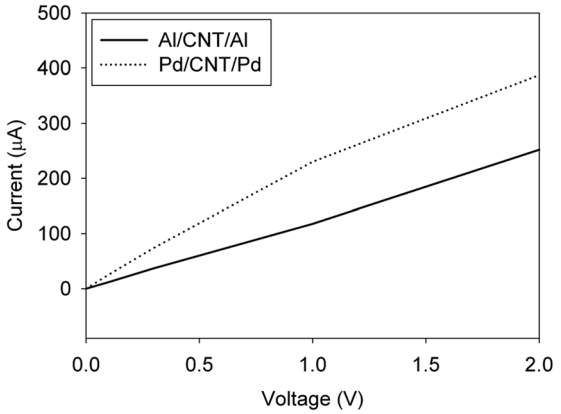

Fig. 6 Current–voltage (*I–V*) curve of Al/CNT/Al and Pd/CNT/Pd systems

Conclusions

Two metal electrodes, namely Al and Pd, were used to form end-contact with an open-end CNT. The Mulliken Overlap Population (MOP) results show that a stronger chemical bond is formed at the Al/CNT interface than at the Pd/CNT interface. However, the Pd/CNT/Pd system shows better electron transport and lower contact resistance. We conclude from these results that there is generally no positive correlation between the charge transfer and the electron transport at the CNT/metal interface.

Acknowledgment

The financial support from Rockwell Collins Inc. is gratefully acknowledged.

References

[1] Rueckes, T., Kim, K., Joselevich, E., Tseng, G. Y., Cheung C. L., and Lieber C. M., 2000, "Carbon Nanotube-Based Nonvolatile Random Access Memory for Molecular Computing," Science, **289**, pp. 94–97.
[2] Zhu, W. G., and Kaxiras, E., 2006, "The Nature of Contact Between Pd Leads and Semiconducting Carbon Nanotubes," Nano Lett., **6**, pp. 1415–1419.
[3] Dag, S., Gulseren, O., Ciraci, S., and Yildirim, T., 2003, "Electronic Structure of the Contact Between Carbon Nanotube and Metal Electrodes," Appl. Phys. Lett., **83**, pp. 3180–3182.
[4] Matsuda, Y., Deng, W.-Q., and Goddard, W. A., 2007, "Contact Resistance Properties Between Nanotubes and Various Metals From Quantum Mechanics," J. Phys. Chem. C, **111**, pp. 11113–11116.
[5] Matsuda, Y., Deng, W.-Q., and Goddard, W. A., 2008, "Improving Contact Resistance at the Nanotube-Cu Electrode Interface Using Molecular Anchors," J. Phys. Chem. C, **112**, pp. 11042–11049.
[6] Meng, T. Z., Wang, C.-Y., and Wang, S.-Y., 2007, "First-Principle Study of Contact Between Ti Surface and Semiconducting Carbon Nanotube," J. Appl. Phys., **102**, p. 013709.
[7] Park, N., and Hong, S., 2005, "Electronic Structure Calculations of Metal-Nanotube Contacts With or Without Oxygen Adsorption," Phys. Rev. B, **72**, p. 048408.
[8] Andriotis, A. N., and Menon, M., 2007, "Structural and Conducting Properties of Metal Carbon-Nanotube Contacts: Extended Molecule Approximation," Phys. Rev. B, **76**, p. 045412.
[9] Andriotis, A. N., and Menon, M., 2008, "Electronic Transport in Metal-Soldered Carbon-Nanotube Multiterminal Junctions," Phys. Rev. B, **78**, p. 235415.
[10] Zhu, L., Hess, D. W., and Wong, C. P., 2006, "In-Situ Opening Aligned Carbon Nanotubes and Applications for Device Assembly and Filed Emission," *Proceedings of 2006 Optics Valley of China International Optoelectronic Exposition and Forum*, pp. 12–18.
[11] Palacios, J. J., Perez-Jimenez, A. J., Louis, E., SanFabian, E., and Verges, J. A., 2003, "First-Principle Phase-Coherent Transport in Metallic Nanotubes With Realistic Contacts," Phys. Rev. Lett., **90**, p. 106801.
[12] Taylor, J., Guo, H., and Wang, J., 2001, "Ab Initio Modeling of Quantum Transport Properties of Molecular Electronic Devices," Phys. Rev. B, **63**, p. 245407.
[13] Odbadrakh, K., Pomorski, P., and Roland, C., 2006, "Ab initio Band Bending, Metal-Induced Gap States, and Schottky Barriers of a Carbon and a Boron Nitride Nanotube Device," Phys. Rev. B, **73**, p. 223402.
[14] Gompernolle, S., Pourtois, G., Soree, B., Magnus, W., Chibotar, L. F., and Ceulemans, A., 2008, "Conductance of a Copper-Nanotube Bundle Interface: Impact of Interface Geometry and Wave-Function Interference," Phys. Rev. B, **77**, p. 193406.
[15] Pomorski, P., Roland, C., and Guo, H., 2004, "Quantum Transport Through Short Semiconducting Nanotubes: A Complex Band Structure Analysis," Phys. Rev. B, **70**, p. 115408.
[16] Gao, F., Qu, J., and Yao, M., 2010, "Electronic Structure and Contact Resistance at an Open-End CNT and Copper Interface," Appl. Phys. Lett., **96**, p. 102108.
[17] ATK Toolkit, 2008. 10 version, www.quantumwise.com.
[18] Perdew, J. P., Burke, K., and Ernzerhof, M., 1996, "Generalized Gradient Approximation Made Simple," Phys. Rev. Lett., **77**, pp. 3865–3868.
[19] Datta, S., 2005, *Quantum Transport: Atom to Transistor*, Cambridge University Press, Cambridge, UK.
[20] Glassey, W. V., and Hoffmann, R., 2000, "A Comparative Study of Hamilton and Overlap Population Methods for the Analysis of Chemical Bonding," J. Chem. Phys., **113**, pp. 1698–1704.
[21] Greenwood, N. N., and Earnshaw, A., 1997, *Chemistry of the Elements*, 2nd ed., Butterworth-Heinemann, Oxford.
[22] Yam, C. Y., Mo, Y., Wang, F., Li, X. B., Chen, G. H., Zheng, X., Matsuda, Y., Tahir-Kheli, J., and Goddard, W. A., 2008, "Dynamic Admittance of Carbon Nanotube-Based Molecular Electronic Devices and Their Equivalent Electric Circuit," Nanotechnology, **19**, p. 495203.